# EFFECT OF TiO2 NANOPARTICLES IN NI MATRIX ON MECHANICAL AND CORROSION RESISTANCE PROPERTIES

*Shahnez Saied*[1)], *Amer Mekkaoui*[1)], *Okba Belahssen*[1)*], *Abdelouahad Chala*[1)]
[1)] *Physic Laboratory of Thin Films and Applications (LPCMA), University of Biskra, Algeria*

Received: 04.12.2016
Accepted: 30.01.2017

[*]Corresponding author: *e-mail:bel_okba@yahoo.fr, Tel.:+213774637626, Physic Laboratory of Thin Films and Applications (LPCMA), University of Biskra, BP 145 RP, 07000 Biskra, Algeria*

## Abstract

Nickel (Ni) is one of the most important hard coatings. Improvement in its tribological and mechanical properties would greatly enhance its use in industry. Nanocomposite coatings of metals with various reinforced nanoparticles have been developed in last few decades. Titania ($TiO_2$) exhibit excellent mechanical properties. It is believed that $TiO_2$ incorporation in Ni matrix will improve the properties of Ni coatings significantly. The main purpose of the current work is to investigate the mechanical and anti-corrosion properties of the electroplated Nickel nanocomposite with a different percentage of $TiO_2$. The results showed that the content of $TiO_2$ and the microhardness in the Ni-$TiO_2$ coatings first increased and reached the maximum at the loading of 20 g/L, then decreased, due to agglomeration of dioxide of Titania for high concentration of $TiO_2$. The [200] preferred orientation for Ni pure gradually evolved to [111] orientation with increasing $TiO_2$ nanoparticle loading. At 20 g/L of titania, we obtained the minimum crystallite size (27 nm). The anti-corrosion property of nanocomposite coating was carried out in 3.5 % NaCl electrolyte, and the result also showed that the nanocomposite coatings improve the corrosion resistance significantly. This present work reveals that incorporation of $TiO_2$ in nickel nanocomposite coating improves corrosion resistance and mechanical properties of both hardness and corrosion resistance performances, and the improvement becomes at it maximum for 20 g/L of $TiO_2$.

**Keywords:** electrodeposition, Ni-$TiO_2$, corrosion, microhardness, mechanical properties

## 1 Introduction

Since the late1990s, metal–ceramic composite coatings have been used on automobile parts, appliances, metal furniture, beverage containers, fasteners, and various other industrial products [1-3]. Composite coatings are formed by components with characteristic dimensionality, such as micro/manometer-size setting in different matrixes [4]. Electrodeposition is a technique for the preparation of excellent performance composite coatings. A characteristic feature of this process is that ceramic particles (ex. SiC, CNTs, TiN, and $TiO_2$) suspended in a liquid medium migrate under the influence of an electric field (electrophoresis) and are deposited on an electrode. All charged ceramic particles used to form stable suspensions can be used in electrodeposition. However, electrodeposition is affected by parameters such as current density, particle concentration, and bath temperature. For example, Bebea and al. [5] found that Co–$ZrO_2$ composite coatings were uniform and well bonded to the substrate, and the thickness of the coating increased with increasing current density. Xia and al. [6] demonstrated that the TiN nanoparticles

DOI 10.12776/ams.v23i1.846

that entered and homogeneously dispersed in a composite coating increased the number of nuclei for nucleation of Ni grains and inhibition of grain growth. Parida and al. [7] reported a Ni– $TiO_2$ composite coating on steel substrates directly prepared by electrodeposition from a bath containing a dispersion of $TiO_2$ power in Watt's bath. $TiO_2$ particles less than 100 nm in size were homogeneously co-deposited with Ni on steel substrate, and microhardness values increased after incorporation of $TiO_2$ compared with a pure Ni deposition.

## 2 Experimental procedure

Pure nickel coating and Ni– $TiO_2$ composite coatings were fabricated on mild steel substrate by electrodeposition. The electrolyte was the traditional Watts bath (**Table 1**). The electrolytes were prepared by adding a range of loadings of 15, 20 and 25 g/L of constituent $TiO_2$ nanoparticles (50 nm) in Watts's bath, respectively. During electrodeposition, pure nickel, and mild steel worked as an anode and a cathode. All the coatings were electrodeposited with the direct current and deposition time of 30 min. The electrolyte composition and preparation parameters are listed in **Table 1**. Before electrodeposition, the mild steel specimens were first polished, and then they were degreased in alkaline solution (NaOH 15 g/L + $Na_2CO_3$ 50 g/L) for 10 min and rinsed in deionized water. After that, they were pickled in 10% HCl solution to remove oxide traces and followed by another rinse in deionized water. The electrolyte was magnetically stirred for 12 h to disperse the nanoparticles. After electrodeposition, the prepared specimens were cleaned with deionized water.

The morphology and chemical composition were characterized by Field Emission Scanning Electron Microscopy (FSEM, JSM-7600 F). Structural investigations phase compositions of the coatings were analyzed by XRD method using a Bruker diffractometer (D8 advance model) with Cu K radiation (1.5406 Å).

The microhardness was examined by Vickers microhardness tester type Wolpert Wilson Instruments model 402UD under loading 25g and holding 15s, and the average microhardness was calculated from 5 measurements. The mass of the electrodeposits was evaluated by weighing the samples before and after the electrodeposition. The anti- corrosion behavior was investigated by potentiodynamic polarization. Potentiodynamic polarization measurements were conducted by using a standard three-electrode cell with the coated samples as a working electrode, Platinum as auxiliary electrode and saturated calomel Ag/AgCl electrode as a reference electrode. All these electrodes were immersed in 3.5 wt % NaCl electrolyte. This cell was connected at voltalab 20 (PGP201) device working at a scanning rate of 0.5 mV/s and a potential range from -700 to -100 mV. Corrosion rate (mm/y), corrosion potential Ecorr (mV), current density Icorr (mA/cm2) and Tafel slopes (mV/s) were calculated by using Tafel extrapolation technique provided by Volta Master4 software.

**Table 1** Optimized constituents of the bath solution

| | | |
|---|---|---|
| Bath composition (g/l) | $NiCl_2$. $H_2O$ | 23.77 |
| | $NH_4Cl$ | 21.4 |
| | $H_3BO_3$ | 18.54 |
| | $TiO_2$ | 15, 20, 25 |
| Conditions | Current density (A/dm2) | 4 |
| | pH | 4 – 4.5 |
| | Time (min) | 30 |
| | Temperature (°C) | 50 |
| | $TiO_2$ grain size (nm) | 50 |

## 3 Results and discussion

### 3.1 Surface morphology and composition of the coatings

**Fig. 1** shows surface morphologies of the coatings electrodeposited at different $TiO_2$ nanoparticle loadings in the electrolyte. As shown in **Fig. 1**, Ni-$TiO_2$ coating showed a typical regular spherical crystal structure. The results showed that the suspended $TiO_2$ nanoparticle loadings in electrolyte strongly influenced the surface morphology evolution of the coatings.

**Fig, 2** shows that relationship between $TiO_2$ contents and $TiO_2$ concentration of nanoparticles was not linear. It was found that the $TiO_2$ contents first increased then decreased. The maximum value of $TiO_2$ content was obtained for 20g/L. This could be attributed to the agglomeration of $TiO_2$ nanoparticles when the $TiO_2$ content increased significantly [8]. Meanwhile, the agglomeration phenomenon raised the roughness and non-homogeneity of Ni-$TiO_2$ coating [9].

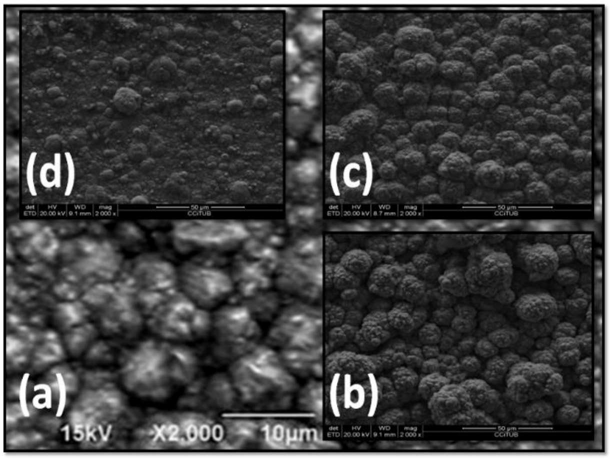

**Fig. 1** Surface morphology of the coating electrodeposited at different $TiO_2$ nanoparticle loadings: (a) 0, (b) 15, (c) 20, (d) 25 g/L

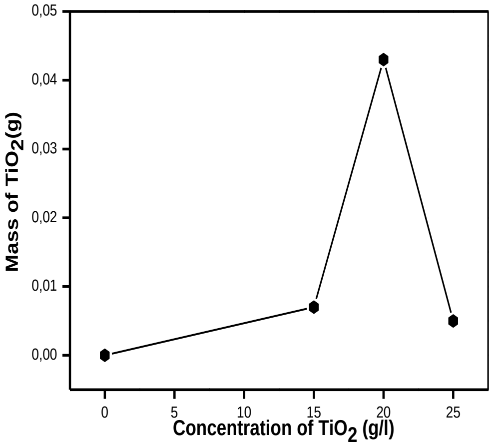

**Fig. 2** Variation of $TiO_2$ contents in the coatings electrodeposited at different concentration of $TiO_2$ nanoparticles

### 3.2 Microstructure and hardness of the coatings

**Fig. 3** compares XRD patterns for the coatings electrodeposited at different $TiO_2$ nanoparticle loadings. The pure Ni coating clearly showed that the relative intensity of the (200) peak was much great. When $TiO_2$ nanoparticle loadings, the relative intensity of the (111) peaks predominated significantly. It could be found that the microstructures of Ni-$TiO_2$ coatings were influenced by the incorporation of $TiO_2$ nanoparticles, implying the crystal orientation evolution of the coatings.

It was recognized that the preferred orientation for the pure Ni coating was [200] orientation in a free Watts bath and would evolve due to the appearance of adsorbed interrupters on the surface of crystallite grain or cathode [5, 10, 11]. McCormack and al. [10] found the $Y_2O_3$ particles in electrolyte contributed to the increase of [111] orientation of Ni-$Y_2O_3$ coating instead of [200] orientation.

This precluded further growth of Ni crystallites. And the adsorbed $TiO_2$ nanoparticles worked as new nucleation sites and shielded the growth sites of Ni ions in the Watts bath. In the case, renucleation of Ni crystallites occurred and the [111] orientation formed.

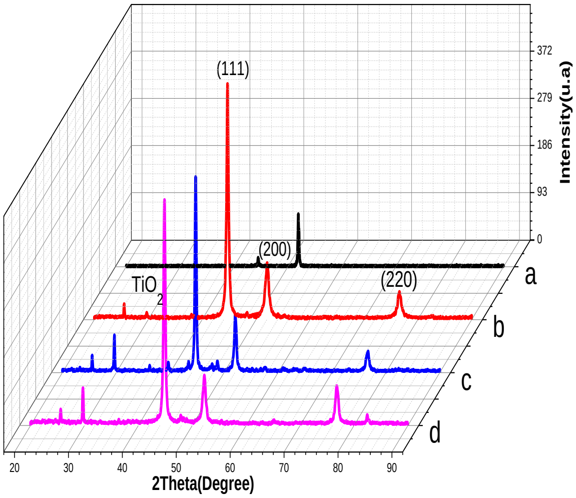

**Fig. 3** XRD patterns of the coating electrodeposition at different $TiO_2$ nanoparticle loadings: (a) 0, (b) 15, (c) 20, (d) 25 g/L

The evolution of crystallite size of the coatings is shown in **Fig. 4**. It demonstrated that crystallite size was strongly dependent on the TiO2 contents in the coatings.

As mentioned above, the incorporated $TiO_2$ nanoparticles precluded the further growth of Ni crystallites and worked as new nucleus sites, then promoted the Ni crystallites refinement. More incorporated $TiO_2$ nanoparticles would induce more Ni crystallites refinement.

Thus, the Ni– $TiO_2$ coating with 20 g/L of $TiO_2$ possessed the smallest crystallite size.

The evolution of microhardness of the coatings is shown in **Fig. 5**. As the $TiO_2$ nanoparticle loadings increased from 0 to 20 g/L, the microhardness increased from 239 to 553.4 HV25. However, the microhardness decreased to 421 HV25 with further increasing the $TiO_2$ nanoparticle loading to 25 g/L. It could be found that the Ni–$TiO_2$ coating with the minimum crystallite size exhibited the maximum microhardness [12, 13, 14].

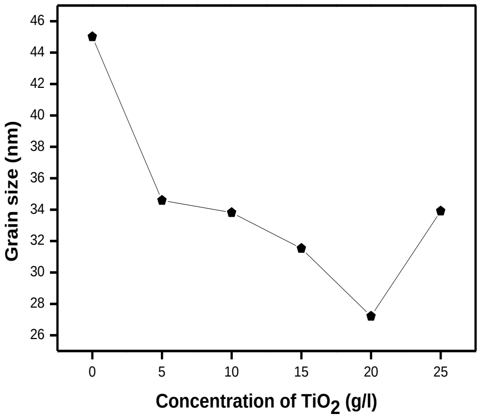

**Fig. 4** Grain size of the coating electrodeposition at different $TiO_2$ nanoparticle loadings

It could be found that the grain size decreased obviously due to the incorporation of $TiO_2$ nanoparticles. And the decreased grain size contributed to the increase of microhardness, which was consistent with Hall–Petch behavior. Generally, dispersion strengthening and grain refinement strengthening are the main mechanisms for strengthening of metal and alloys [15]. Due to the incorporation of $TiO_2$ nanoparticles in Ni-$TiO_2$ coatings, the Ni matrix crystallite size decreased a lot. The grain refinement strengthening mechanism was quite effective for the improvement of microhardness of the Ni-$TiO_2$ coatings. As strong obstacles for dislocation movement, the incorporated $TiO_2$ nanoparticles in Ni matrix contributed to the dispersion strengthening. Thus, the Ni-$TiO_2$ coating electrodeposited at 20 g/L possessed the maximum value of microhardness due to the smallest crystallite size and the most strong [111] orientation.

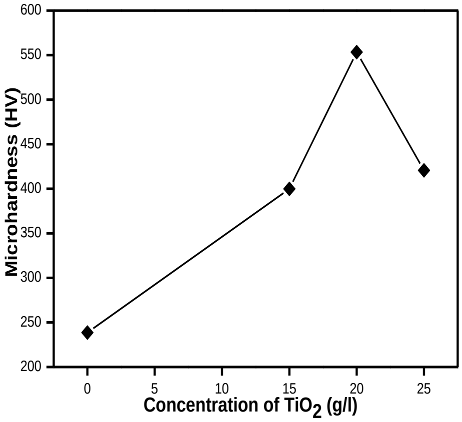

**Fig. 5** Microhardness of the coating electrodeposited at different $TiO_2$ nanoparticle loadings

### 3.3 Corrosion behavior of the coatings

Potentiodynamic polarization curves of the coatings are presented in **Fig. 6**, and the corrosion parameters (corrosion potential Ecorr and Corrosion current Icorr) are presented in **Table 2**. The corrosion potentials of the Ni-$TiO_2$ coatings were higher than that of pure Ni coating. And it could be found that the corrosion current had decreased trend with increasing the $TiO_2$ nanoparticle loading in electrolyte.

In the microstructure evolution, the crystallite size refinement played important roles in the improvement of the anti-corrosion behavior. From **Fig. 7** and **Table 2**, it could be found that the decreased crystallite size enabled the Ni-$TiO_2$ coatings with superior anti-corrosion behavior. This was because that the smaller crystallite size could facilitate the passivation of the nickel matrix [16, 17]. In the FCC crystalline structure of Ni matrix, the dissolution of atoms of the (111) planes needed more energy than that of (200) planes [17]. Therefore, the formation of [111] orientation was beneficial to the anti-corrosion behavior of the Ni-$TiO_2$ coatings. Furthermore, the uniformly distributed nanoparticles in the coating could act as physical barriers [2] to hinder the defect corrosion. Thus, the incorporation of $TiO_2$ nanoparticles was beneficial to the anti-corrosion behavior of the Ni-$TiO_2$ coatings.

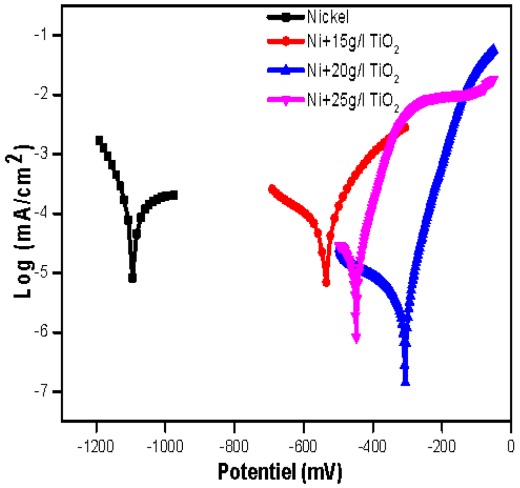

**Fig. 6** Potentiodynamic polarization curves for the coatings electrodeposition at different $TiO_2$ nanoparticle loading

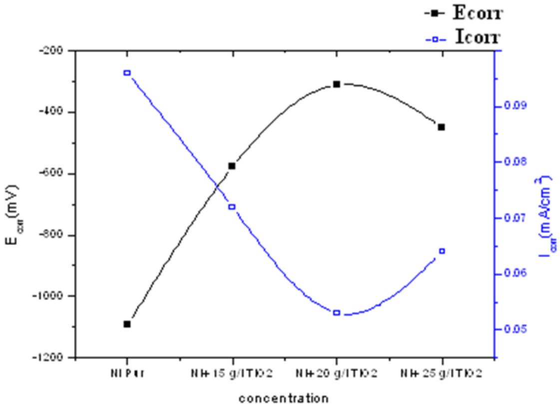

**Fig. 7** Variation of Ecorr and Icorr in the coatings electrodeposited at different $TiO_2$ nanoparticle loadings

**Table 2** Optimized constituents of the bath solution

| | bc (mV) | ba (mV) | Ecorr (mV) | Icorr (mA/cm$^2$) | Rp (ohm.cm$^2$) |
|---|---|---|---|---|---|
| Ni pure | -71.00 | 10.90 | -1094 | 0.096 | 2529 |
| Ni+ 15g/L $TiO_2$ | -196.30 | 14.12 | -578 | 0.072 | 3018 |
| Ni+ 20g/L $TiO_2$ | -179.50 | 43.40 | -312 | 0.053 | 6118 |
| Ni+ 25g/L $TiO_2$ | -190.03 | 48.00 | -449.9 | 0.064 | 1120 |

## Conclusions

Ni-$TiO_2$ nanocomposite coatings were fabricated by electro deposition in watts bath. $TiO_2$ nanoparticles reinforced Ni nanocomposite coatings revealed a much smoother and compact surface microstructure with excellent mechanical properties. Meanwhile, the corrosion resistance has been enhanced significantly. Effectively, the incorporated $TiO_2$ nanoparticles precluded the further growth of Ni crystallites and worked as new nucleus sites, then promoted the Ni crystallites refinement. The crystallite size refinement played important roles in the improvement of the microstructure, microhardness and anti-corrosion behavior of Ni-$TiO_2$ nanocomposite coatings. The Ni-$TiO_2$ coating electrodeposited at 20 g/L of $TiO_2$ possessed the maximum value of hardness and a good tendency for corrosion resistance.

## References

[1] H. Schmidt, S. Langenfeld, R. Naß: A new corrosion protection coating system for pressure-cast aluminium automotive parts, Materials and design, Vol. 18, 1997, No. 3, p. 309–313, DOI: 10.1016/S0261-3069(97)00070-8

[2] R.I. Amaro, R. C. Martins, J. O. Seabra, N. M. Renevier, D. G. Teer: Molybdenum disulphide / titanium low friction coating for gears application, Tribology International, Vol. 38, 2005, No. 4, p. 423–434, DOI: 10.1016/j.triboint.2004.09.003

[3] A. Naci Tankut, N. Tankut: Investigations the effects of fastener glue and composite material types on the strength of corner joints in case-type furniture construction, Materials and design, Vol. 30, 2009, No. 10, p. 4175–4182, DOI: 10.1016/j.matdes.2009.04.038

[4] F.F. Xia, H. B. Xu, C. Liu, J. W. Wang, J. J. Ding, C. H. Ma: Micro-structures of Ni-AlN composite coatings prepared by pulse electrodeposition technology, Applied Surface Science, Vol. 271, 2013, p. 7–11, DOI: 10.1016/j.apsusc.2012.12.064

[5] L. Bebea, P. Ponthiaux, F. Wenger: Co-ZrO2 electrodeposited composite coatings exhibiting improved microhardness and corrosion behavior in simulating body fluid solution, Surface and Coatings Technology, Vol. 205, 2011, p. 5379–5386, DOI: 10.1016/j.surfcoat.2011.05.050

[6] F. Xia, M. Wu, F. Wang, Z. Jia, A. Wang: Nanocomposite Ni-TiN coatings prepared by ultrasonic electrodeposition, Current Applied Physics, Vol. 9, 2009, p. 44–47 http://dx.DOI.org/10.1016/j.cap.2007.11.014

[7] G. Parida, D. Chaira, M. Chopkar, A. Basu: Synthesis and characterization of Ni–TiO2 composite coatings by electro-co-deposition, Surface and Coatings Technology , Vol. 205, 2011, p. 4871–4879, DOI: 10.1016/j.surfcoat.2011.04.102

[8] V. Hasannaeimi, T. Shahrabi, S. Sanjabi: Fabrication of NiTi layer via electrodeposition of nickel and titanium, Surface and Coatings Technology, Vol. 210, 2012, p. 10–14, DOI: 10.1016/j.surfcoat.2012.07.054

[9] D. Eroglu, A. Vilinska, P. Somasundaran, A. C. West: Use of dispersants to enhance incorporation rate of nano-particles into electrodeposited films, Electrochimica Acta, Vol. 113, 2013, p. 628–634, DOI: 10.1016/j.electacta.2013.09.113

[10] A. G. McCormack, M. J. Pomeroy, V. J. Cunnane: Microstructural development and surface characterization of electrodeposited nickel-yttria composite coatings, Journal of The Electrochemical Society, Vol. 150, 2003, p. 356–361, DOI:10.1149/1.1566961

[11] J. Amblard, I. Epelboin,M. Froment, G. Maurin: Inhibition and nickel electro crystallization, Journal of Applied Electrochemistry , Vol. 9, 1979, p. 233–242, DOI: 10.1007/BF00616093

[12] F. Y. Hou, W. Wang, H. T. Guo: Effect of the dispersibility of ZrO2 nanoparticles in Ni-ZrO2 electroplated nanocomposite coatings on the mechanical properties of nanocomposite coatings, Applied Surface Science, Vol. 252, 2006, p. 3812–3817, DOI: 10.1016/j.apsusc.2005.05.076

[13] C. T. Chen, Y. C. Song, G. P. Yu, J. H. Huang: Microstructure and hardness of hollow cathode discharge ion-plated titanium nitride film, Journal of Materials Engineering and Performance, Vol. 7, 1998, p. 324–328, DOI: 10.1361/105994998770347756

[14] L. P. Wang, J. Y. Zhang, Y. Gao, Q. J. Xue, L. T. Hu, T. Xu: Grain size effect in corrosion behavior of electrodeposited nanocrystallite Ni coatings in alkaline solution, Scripta Materialia, Vol. 55, 2006, p. 657–660, DOI: 10.1016/j.scriptamat.2006.04.009

[15] R. Mishra, R. Balasubramaniam: Effect of nanocrystallite grain size on the electrochemical and corrosion behavior of nickel, Corrosion Science, Vol. 46, 2004, p. 3019–3029, DOI: 10.1016/j.corsci.2004.04.007

[16] J.C. Scully: The Fundamentals of Corrosion, Pergamon Press, 1990, DOI: 10.1002/maco.19910420115

[17] Y. Zhao, C. Jiang, Z. Xu: Microstructure and corrosion behavior of nanoparticles reinforced Ni-Ti composite coatings by electrodeposition, Materials and design , Vol. 85, 2015, p. 39–46, DOI: 10.1016/j.matdes.2015.06.144